

## Mechanical and thermal characterization of *cis*-polyisoprene and *trans*-polyisoprene blends

Mahesh Baboo · Manasvi Dixit · Kananbala Sharma ·  
Narendra S. Saxena

Received: 6 May 2010 / Revised: 14 July 2010 / Accepted: 15 September 2010 /  
Published online: 29 September 2010  
© Springer-Verlag 2010

**Abstract** Measurements of mechanical and thermal transport properties have been made on the blends of *cis*-polyisoprene (CPI) and *trans*-polyisoprene (TPI) prepared by a solution casting method. Characterization of these blends has been done using wide angle X-ray scattering. Thermo-mechanical, mechanical, and thermal transport properties have been determined employing dynamic mechanical analyzer (DMA) and transient plane source. Storage modulus and  $\tan \delta$  as determined from DMA have been found to increase and decrease with the increase in TPI content, respectively. Mechanical properties such as Young's modulus and tensile strength, as determined from strain–stress behavior of CPI/TPI blends, have been found to increase with increasing TPI content. This increase in properties has been explained on the basis of the crosslink density, calculated using theory of rubber elasticity. Thermal transport properties such as thermal conductivity, thermal diffusivity, and volumetric heat capacity are higher for all the three blends as compared to their pure components.

**Keywords** Elastomer · Glass-transition · Mechanical property · Thermal conductivity · Crosslink density · Crystallinity

### Introduction

The technique of blending of two or more elastomers to produce an end product having a combination of properties has gained significant industrial information

---

M. Baboo (✉) · M. Dixit · K. Sharma · N. S. Saxena (✉)  
Semiconductor and Polymer Science Laboratory, University of Rajasthan, 5-6, Vigyan Bhawan,  
Jaipur 302 004, India  
e-mail: m.baboo@rediffmail.com

N. S. Saxena  
e-mail: n\_s\_saxena@rediffmail.com

nowadays. The properties of elastomeric blends are affected by factors [1, 2] like the molecular weight, the thermodynamic compatibility, crosslink density, and crystallinity of the elastomers.

Cooper and Vaughan [3] have used *cis*-polyisoprene (CPI) and *trans*-polyisoprene (TPI) blends and have reported that a mixture of CPI and TPI causes a marked reduction in the rate of crystallization of CPI. Bhowmick et al. [4] found that TPI did not act as a nucleating site for crystallization of CPI. Strain-induced crystallization (SIC) in blends of CPI and TPI was studied by Manzur [5] and results showed that the presence of TPI in CPI promoted the SIC and seemed to indicate that the number of nucleation sites increased with increasing TPI content. More recently, Boochathum et al. [6, 7], in two different studies, reported the cure characteristics, crosslink distribution, crystallization characteristics, and properties. The influence of crystallinity on the glass transition temperature of TPI/liquid CPI blends has also been investigated by Baboo et al. [1] and the results showed that  $T_g$  increases with decreasing crystallinity.

This article reports the effect of blending of CPI with TPI in terms of crosslink density and crystallinity on thermo-mechanical properties like  $\tan \delta$  and storage modulus, mechanical properties like Young's modulus, tensile strength and toughness, and thermal transport properties like thermal conductivity ( $\lambda$ ), thermal diffusivity ( $\chi$ ), volumetric heat capacity ( $\rho c_p$ ).

## Experimental

### Preparation of samples

The basic materials used in this study are CPI, which is in rubbery lump form and TPI, which is in granular form, and were obtained from Sigma-Aldrich, Japan.

Both CPI and TPI of known polymer compositions were separately dissolved in toluene and then mixed in the TPI/CPI weight ratio of 100/0, 75/25, 50/50, 25/75, and 0/100. The solutions were slowly cast on Petri dish and kept for drying in air for a period of 2–3 weeks. To ensure that the sample did not contain solvent, the films were further dried in vacuum for 2 days at ambient temperature. Films were prepared with the  $\sim 2.5$  mm thickness for all blends. Uniformity of the thickness of the film has been ensured by measuring the same at different points of the film.

### Characterization

Wide angle X-ray scattering (WAXS) measurements were carried out on a Philips X'pert X-ray diffractometer using copper target ( $\text{Cu } K_\alpha$ ) at a scanning rate of  $3^\circ$  per minute between  $10^\circ$  and  $60^\circ$ . All the data were recorded in reflection mode.

Thermal transport properties have been determined by means of transient plane source (TPS) technique. Detailed theory of this method is described further in this article.

Mechanical properties have been measured using dynamic mechanical analyzer (DMA). This is a sensitive technique that characterizes the mechanical response of

materials by monitoring property changes with respect to the temperature and frequency of an applied sinusoidal stress. With the use of this technique, a force is applied to the sample and the amplitude and phase of the resulting displacement are measured. The details of the technique are discussed elsewhere [8]. For DMA measurements, film samples were cut into 4.5 mm width and 8.05 mm length and were applied in tension mode.

## Theory

### Determination of crystallinity

The degree of crystallinity,  $X_c$ , and amorphous content,  $X_a$ , have been calculated using the following relationship:

$$X_c = I_c / (I_a + I_c), \quad X_a = I_a / (I_a + I_c) \quad (1)$$

where  $I_c$  and  $I_a$  are the integrated intensities of the crystalline and the amorphous phase, respectively, which can be determined by drawing the line of demarcation in such a manner as to be congruent with the spectrum profile of the blend [9]. In this usual method, the area above the demarcation curve is taken to be proportional to the intensity of crystalline scattering,  $I_c$ , and the area between the baseline and the demarcation curve is taken to be proportional to the intensity of amorphous scattering,  $I_a$ . The interplanar distance ( $d$ ) was calculated as follows:

$$d = \lambda / 2 \sin \theta \quad (2)$$

where  $\lambda$  is the wavelength (1.540 Å for Cu) of the X-ray radiation.

### Determination of crosslink density

Crosslink density is an important parameter which influences the thermo-mechanical properties of elastomeric blends. The crosslink density ( $\rho$ ) has been determined according to the theory of rubber elasticity as follows [10]

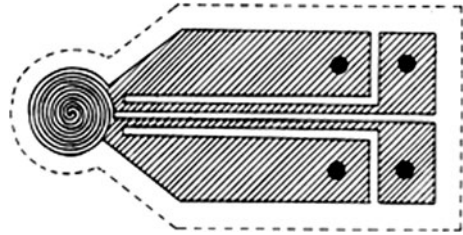
$$\rho = G / 3\phi RT \quad (3)$$

where  $G$  is the storage modulus at  $T_g + 50^\circ \text{C}$ ,  $\phi$  a front factor (assumed as  $\phi = 1$ ),  $R$  the gas constant, and  $T$  the absolute temperature at  $T_g + 50^\circ \text{C}$ .

### Determination of thermal transport properties

Thermal transport properties of CPI/TPI at different temperatures were determined using the TPS method [11]. In this method, the TPS element behaves both as temperature sensor and heat source. TPS element (Fig. 1) consists of an electrical conducting pattern of thin nickel foil (10  $\mu\text{m}$ ) in the form of double spiral embedded in an insulating layer made of kapton (70  $\mu\text{m}$ ). Sensor is sandwiched between the two pieces of the samples having perfectly smooth surface so as to ensure perfect thermal contact.

**Fig. 1** Schematic diagram of TPS sensor



A constant electrical power is supplied to the sensor and the increase in temperature  $\Delta T(\tau)$  is calculated from the variation in the resistance of the sensor using the equation:

$$\Delta T(\tau) = 1/\alpha \{ [R(T)/R_0] - 1 \} \quad (4)$$

where  $R_0$  is resistance of the hot-disk in the beginning of the recording (initial resistance),  $\alpha$  the temperature coefficient of resistance of the nickel foil, and  $\Delta T(\tau)$  the temperature increase in the sensor expressed in terms of a variable  $\tau$ , defined as:

$$\tau = (t/\theta)^{1/2}, \quad \theta = a^2/\chi \quad (5)$$

where  $t$  is the measurement time,  $\theta$  the characteristic time, which depends on both of parameters of the sensor ( $a$  is the sensor radius) and the thermal diffusivity ( $\chi$ ) of the sample.

Assuming the conductive pattern to be in the  $Y$ - $Z$  plane of a coordinate system, the temperature rise at a point  $(y, z)$  at time  $t$  due to an output of power per unit area  $Q$  is given by the expression:

$$\begin{aligned} \Delta T(y, z, t) = & \frac{1}{8\pi^{3/2}\rho c} \int_0^t dt' [\chi(t-t')]^{3/2} \int_A dy' dz' Q[y', z', t'] \\ & \times \exp \left\{ - \left[ (y-y')^2 + (z-z')^2 \right] \times [4\chi(t-t')]^{-1} \right\} \end{aligned} \quad (6)$$

where  $\rho$  is the density ( $\text{kg/m}^3$ ) of the material and  $c$  is the specific heat of the sample ( $\text{J/kg K}$ ).

Equation 6 can be simplified, taking  $\chi(t-t') = \sigma^2 a^2$ :

$$\Delta T(y, z, \tau) = \frac{1}{4\pi^{3/2}a\lambda} \int_0^\tau \sigma^{-2} d\sigma \int_A dy' dz' Q[y', z', t'] \exp \left[ - \frac{(y-y')^2 + (z-z')^2}{4\sigma^2 a^2} \right] \quad (7)$$

where  $\chi = \lambda/\rho c$  and  $\lambda$  is the thermal conductivity.

In the case of disk geometry, consisting of  $m$  concentric ring sources, an exact solution of Eq. 4 is possible. The average increase in temperature is

$$\Delta T(\tau) = P_o \left( \pi^{3/2} a \lambda \right)^{-1} D(\tau) \tag{8}$$

where  $P_o$  is the total output power and  $D(\tau)$  is a geometric function given by the following expression:

$$D(\tau) = [m(m + 1)]^{-2} \times \int_0^\tau \frac{d\sigma}{\sigma^2} \left[ \sum_{l=1}^m l \left\{ \sum_{k=1}^m k \cdot \exp\left(\frac{-l^2 - k^2}{2\sigma^2 m^2}\right) \right\} L_0\left(\frac{lk}{2\sigma^2 m^2}\right) \right] \tag{9}$$

in which  $L_0$  is the modified Bessel function.

Thermal conductivity can be obtained by fitting the experimental data to the straight line given by Eq. 8, and thermal diffusivity is calculated from Eq. 5 taking into account for the  $\tau$  value determined in the previous fit. Finally, heat capacity is derived from the values of  $\lambda$  and  $\chi$  using the relation  $\chi = \lambda/\rho c_p$ .

### Result and discussion

#### Wide angle X-ray scattering

The XRD pattern of pure CPI and pure TPI and their blends are shown in Fig. 2. From the figure, the pure CPI is amorphous, whereas TPI is partially crystalline [5]. The interplanar spacing has been calculated using Eq. 2 and shown in Fig. 2 from which the crystalline form was identified as of the high melting form [5]. It has been reported [12] that in binary systems, the presence of a crystalline polymer (TPI) substantially affects the amorphous character of the other amorphous polymer (CPI).

From Fig. 2, it is also observed that crystalline peaks of TPI continue to be present at the same position of  $2\theta$  for all the compositions. The WAXS

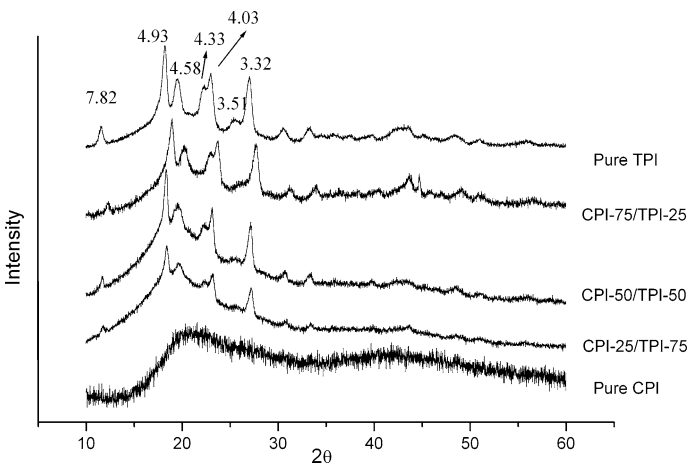


**Fig. 2** WAXS patterns of CPI/TPI blends

measurements also inferred that the percentage of crystallinity calculated using Eq. 1 of the blends increases with the addition of TPI as given in Table 1. This is due to the incorporation of crystalline TPI [5] into CPI, which in turn increases the overall crystallinity of the blend. Thus, TPI does not act as a nucleating agent but contributes its own crystallinity for increasing the overall crystallinity of the blend.

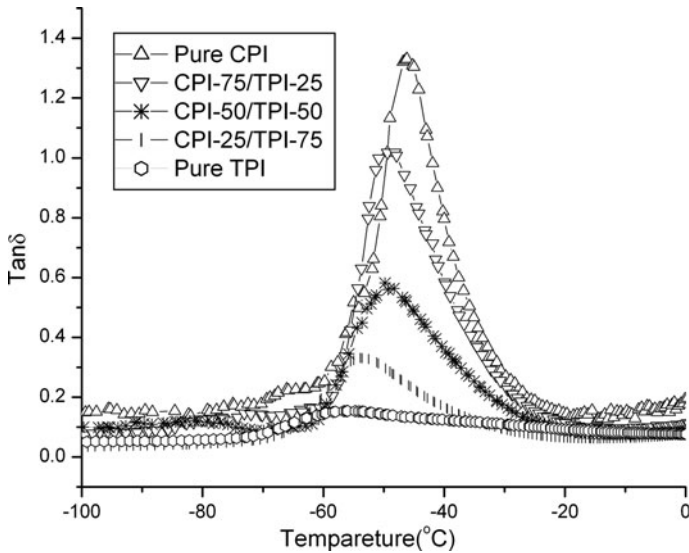
### Thermo-mechanical properties

Figure 3 shows the temperature dependence of loss tangent for different CPI/TPI blends. The plots of  $\tan \delta$  against temperature show well-defined and symmetric peaks corresponding to the relaxation associated to the transition from glassy state to the elastic state of the rubber. The characteristic temperature corresponding to the peak point is identified as glass transition temperature  $T_g$  [1]. All the blends show a single but separate glass transition temperature, which confirm that all the blends are miscible as reported by other researchers [6, 7]. It is observed from this figure that both glass transition temperature and height of  $\tan \delta$  peak are in increasing trend with increasing TPI content. This behavior can be explained on the basis of crosslink density. As the concentration of TPI increases, crosslink density also increases (Table 1) and therefore a rigid structure is produced due to the lower molecular weight between crosslink. As a result, there is a shifting in the transition ( $T_g$ ) to lower temperature observed. Moreover, it is reported [13] that the glass transition temperature depends upon crystallinity. So, this can also be explained on the basis of WAXS measurements. An increase in TPI concentration increases the crystallinity (Table 1) and as a result  $T_g$  shifted to lower side. The height of  $\tan \delta$  peak represents the damping property of the material. An increase in the TPI concentration of the blend produces a rigid structure due to the higher crosslink density. This rigid structure is responsible for the restriction of mobility of the polymer chain. Hence, higher concentration of TPI produces higher restriction of mobility of polymer chains and as a result lowers the damping property.

Figure 4 shows the variation of storage modulus versus temperature. From this figure, it has been observed that there is a small decrement in the value of storage modulus with temperature near up to about  $-60$  °C in all the blends. As the temperature further increases, the storage modulus shows a sharp drop in almost all blends and then attains a constant value in the temperature region from  $-40$  to  $-20$  °C. This phenomenon is due to the fact that the molecules may be considered as a collection of mobile segment that have higher degree of free movement. At a lower temperature, the molecules of the solid material have lower kinetic energies

**Table 1** Values of crosslink density and percentage crystallinity of CPI/TPI blends

Composition (W/W)	% Crystallinity	Crosslink density (mol/m <sup>3</sup> )
Pure CPI	Amorphous	$0.107 \times 10^3$
CPI-75/TPI-25	13.89	$0.523 \times 10^3$
CPI-50/TPI-50	38.68	$3.711 \times 10^3$
CPI-25/TPI-75	40.33	$19.866 \times 10^3$
Pure TPI	65.70	$22.129 \times 10^3$



**Fig. 3**  $\tan \delta$  versus temperature curve of CPI/TPI blends

and their oscillations about their mean position are small; the material is tightly compressed. Therefore, in this state, the lack of free volume restricts the possibility of motion in various directions; hence, the molecules are unable to respond to a load or stress to which the sample is subjected [14, 15]. As a result there is a high value of the modulus. However, at elevated temperature (near about  $T_g$ ), the free volume of the chain segments increases, thereby resulting in an increment of mobility of molecular segments. The motion of these chains produces more strain in the sample with applied load; hence, the modulus of the sample decreases in the temperature range from  $-59$  to  $-46$  °C which is glass transition range for pure TPI and their blends with CPI.

From this figure, it is also clear that the value of storage modulus increases with increasing TPI content. In the temperature range  $-100$  to  $-50$  °C, the value of storage modulus is higher for CPI-25/TPI-75 while it is higher for pure TPI in the temperature range  $-50$  to  $0$  °C. This behavior might be attributed to the different cold crystallizations of CPI-25/TPI-75 blend [6].

### Mechanical properties

The stress–strain curve reflects the whole tensile course of the elastomeric blends which is extremely helpful for understanding the engineering application of the material. Figure 5 represents the stress–strain behavior of CPI and CPI/TPI blends. From Fig. 5 it is clear that the stress–strain features of all the blends are quite different. As the concentration of TPI increases in the CPI/TPI blends, elastic region increases while plastic region decreases. For the blend CPI-25/TPI-75, the stress value is high in the early stage of the strain development and the stress remains constant in plastic region. This behavior (for CPI-25/TPI-75) indicates higher

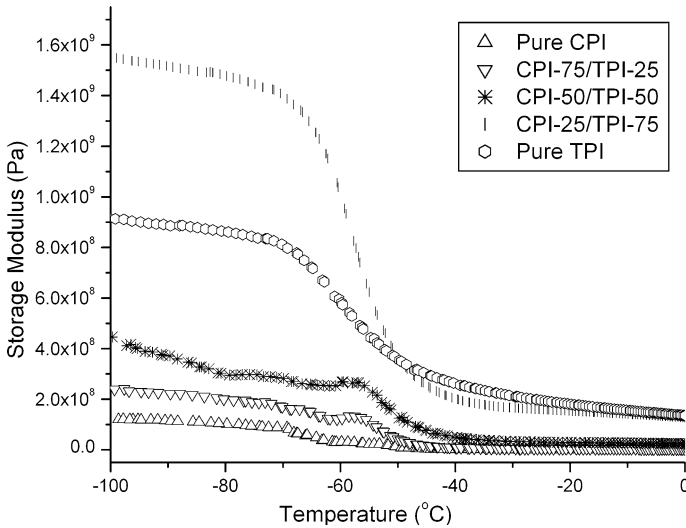


**Fig. 4** Storage modulus versus temperature curve of CPI/TPI blends

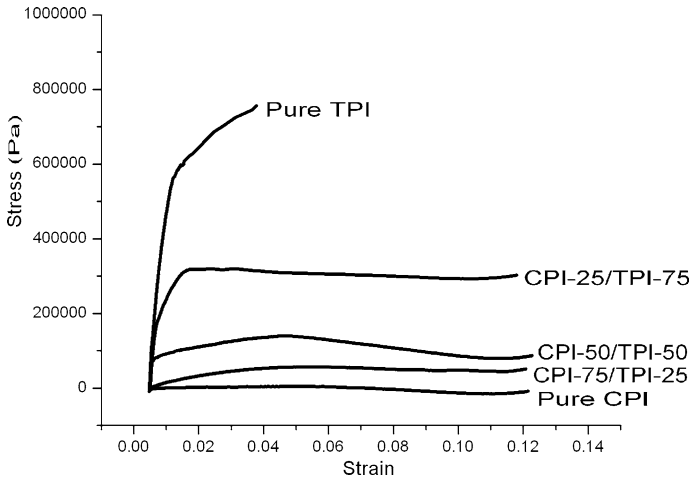


**Fig. 5** Comparison of stress–strain curves of the CPI/TPI blends

toughness of the material consequently higher fracture energy. The stress value for pure TPI shows increasing trend abruptly in the early stage of the strain development while the stress increases with slow rate in the plastic region.

The mechanical properties—toughness, young's modulus, and tensile strength—have been calculated from stress–strain behavior of curves and are given in Table 2. Both stress–strain behaviors and mechanical properties can be explained on the basis of crosslink density. As the concentration of TPI increases in the blends of CPI/TPI, the crosslink density also increases (Table 1) and consequently the



**Table 2** The comparison of mechanical properties of the samples

Composition (W/W)	Young’s modulus (Pa)	Tensile strength (Pa)	Toughness (J/m <sup>3</sup> )
Pure CPI	0.355E6	0.498E4	2.15E2
CPI-75/TPI-25	1.616E6	6.418E4	4.36E3
CPI-50/TPI-50	1.390E7	1.481E5	6.01E3
CPI-25/TPI-75	1.126E8	3.237E5	3.42E4
Pure TPI	1.804E8	7.837E5	2.01E4

material is more tightly bound. Therefore, the restricted chain mobility reduces the ability of the chain to respond to a load or stress to which the sample is subjected [13] and both tensile strength and young’s modulus are higher.

Thermal transport properties

Figure 6 shows the thermal conductivity and thermal diffusivity values plotted against composition of the CPI/TPI blends. Thermal conductivity of pure CPI and pure TPI is almost equal. As the concentration of TPI increases in the CPI/TPI blend, the thermal conductivity increases. This fact can be explained on the basis of crystallinity and crosslink density. It has been reported [14] that an increase in crystallinity increases the thermal conductivity. In this samples, an increase in the TPI content of CPI/TPI blend increases both crystallinity and crosslink density which in turn increases the thermal conductivity of the samples. This is due to the fact that an increase in crosslink density decreases the average distance between the crosslinks. Further increment in crosslink density reduces the average distance between crosslinks or chains up to a certain limit; after this limit, a stage comes when these crosslinks or chains unite together resulting in an abrupt increase in

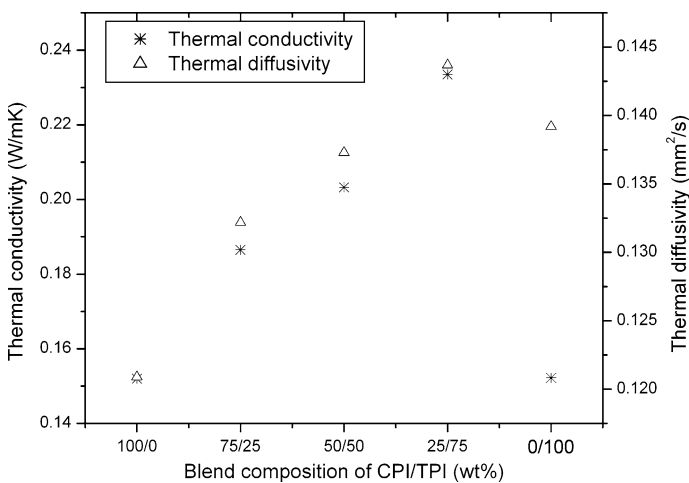


**Fig. 6** Thermal conductivity and thermal diffusivity versus blend composition

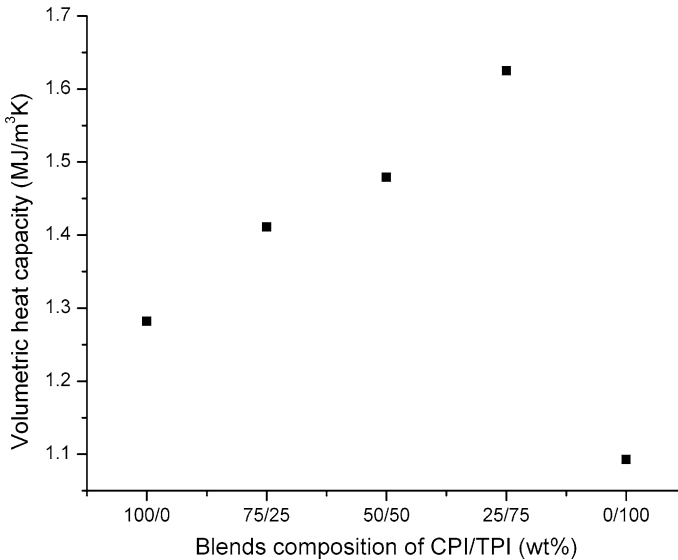


**Fig. 7** Volumetric heat capacity versus blend composition

average distance between them [15]. According to Berman et al. [16], if the average distance between the crosslinks is less than the range of elastic disorder (10 Å), thermal conductivity continuously increases with increasing crosslink density (which is in the case of CPI-75-TPI-25, CPI-50-TPI-50, and CPI-25-TPI-75 blends). In the case where average distance between crosslinks is greater than the range of elastic disorder, thermal conductivity is seemed to decrease with increasing crosslink density (which is the case of pure TPI). Morgan and Scovell [17] proposed a postulate to this phenomenon. They postulated the existence of one-dimensional wave packets, which travel along the chains and have long mean-free paths. The wave packets may be scattered by chain ends, crosslinks, or interactions with other molecules, which reduces the thermal conductivity. Thermal diffusivity ( $\chi$ ) of the blends exhibits the same trend as obtained in the case of the thermal conductivity values, showing the proportionality between  $\lambda$  and  $\chi$ . Figure 7 shows the volumetric heat capacity ( $\rho c_p$ ) of the CPI/TPI blends. From this figure, it is observed that  $\rho c_p$  for pure CPI and pure TPI are 1.28 and 1.09, respectively. As the concentration of TPI increases in CPI/TPI blends,  $\rho c_p$  increases and it is observed to be highest for CPI-25/TPI-75.

## Conclusions

The mechanical and thermal transport properties of CPI and/or TPI have been investigated in relation to weight ratio of the CPI and TPI in the blend. From these experimental results, the following conclusions can be drawn:

1. The increasing trend of crystallinity with increasing TPI content shows that TPI does not act as a nucleating agent for CPI and the increment in crosslink density values shows that TPI acts as inert filler for CPI.
2. Both elastic modulus and tensile strength are increased with increasing TPI composition in the blends. However, the CPI-25/TPI-75 blend shows higher fracture energy. This is consistent with the crosslink density values and effective average chain length of the blend.
3. All the three thermal transport properties—thermal conductivity, thermal diffusivity, and volumetric heat capacity—are increased with increasing TPI content. However, pure TPI shows lower thermal properties than that of the blends but higher than that of pure CPI. This variation in thermal transport properties confirms that not only crystallinity, but also crosslink density and effective average chain length are responsible for these properties.
4. This study shows that the CPI-25/TPI-75 blend is more useful than the other two blends in engineering application where a material having higher thermal properties with good mechanical properties is needed.

**Acknowledgments** One of the authors thankful to the BRNS (DAE), Government of India for the financial support vide Grant No. 2007/37/49/BRNS sanctioned to Prof. Kananbala Sharma and Prof. N. S. Saxena. Mahesh Baboo and Manasvi Dixit are also thankful to Ms. Deepika and Ms. Sonalika Agrawal for their help in various ways during the course of the study.

## References

1. Baboo M, Dixit M, Sharma KB, Saxena NS (2009) The structure and thermomechanical properties of blends of *trans*-polyisoprene with *cis*-polyisoprene. *Int J Polym Mater* 58:636–646
2. Fried JR (1999) Polymer science and technology. Prentice Hall, New Delhi
3. Cooper W, Vaughan G (1963) Crystallization of gutta percha and synthetic *trans*-1,4-polyisoprenes. *Polymer* 4:329–340
4. Bhomic AK, Kuo CC, Manjur AMAC, Arthur AMC, Intyre D (1986) Properties of *cis*- and *trans*-polyisoprene blends. *J Macromol Sci Phys B* 25:283–306
5. Manzur A (1989) Strain-induced crystallization in *cis*- and *trans*-polyisoprene blends: apparent crystallinity. *J Macromol Sci Phys B* 28:329–337
6. Bochathum P, Chuwnawin S (2001) Vulcanization of *cis*- and *trans*-polyisoprene and their blends: crystallization characteristics and properties. *Eur Polym J* 37:429–434
7. Boochathum P, Prajudtake W (2001) Vulcanization of *cis*- and *trans*-polyisoprene and their blends: cure characteristics and crosslink distribution. *Eur Polym J* 37:417–427
8. Dixit M, Shaktawat V, Saxena NS, Sharma KB, Sharma TP (2008) Mechanical characterization of polymethyl methacrylate and polycarbonate blends. *AIP Proc* 1004:311–315
9. Alexander LE (1979) X-ray diffraction methods in polymer science. Huntington, New York
10. Kaji M, Nakahara K, Endo T (1999) Synthesis of a bifunctional epoxy monomer containing biphenyl moiety and properties of its cured polymer with phenol novolac. *Appl Polym Sci* 741:690–698
11. Gustafsson SE (1991) Transient plane source techniques for thermal conductivity and thermal diffusivity measurements of solid materials. *Rev Sci Instrum* 62:797–804
12. Arvanitoyannis I, Kolokuris I, Nakayama A, Aiba S (1997) Preparation and study of novel biodegradable blends based on gelatinized starch and 1,4-*trans*-polyisoprene (gutta percha) for food packaging or biomedical applications. *Carbohydr Polym* 34:291–302
13. Shaktawat V, Jain N, Saxena NS, Sharma KB, Sharma TP (2007) Thermomechanical investigation of a thick film of aniline-formaldehyde copolymer and poly(methyl methacrylate). *Polym Sci B* 49:236–239

14. Jayasree TK, Predeep P, Agarwal R, Saxena NS (2006) Thermal conductivity and thermal diffusivity of thermoplastic elastomeric blends of styrene butadiene rubber/high density polyethylene: effect of blend ratio and dynamic crosslinking. *Trends Appl Sci Res* 1:278–291
15. Evseeva LE, Tanaeva SA (1995) Thermophysical properties of epoxy composite materials at low temperatures. *Cryogenics* 35:277–279
16. Berman BL, Madding RP, Dellinger JR (1969) Effect of crosslinking on the thermal conductivity of polystyrene between 0.3 K and 10 K. *Phys Lett A* 30:315–316
17. Morgan GJ, Scovell PD (1977) Effective conductivity of short carbon fiber-reinforced polychloroprene rubber and mechanism of conduction. *Polym Lett* 15:193